birge is an anticlinal structure with an ellipsoidal shape, extending in a WSW-ENE direction (Fig. 2). It is surrounded by anchimetamorphic to low-grade metamorphic rocks. Towards the south the crystalline complex of the Erzgebirge is limited by the Eger graben (the river Eger is named Ohře in Czech), which is a Late Cretaceous to Tertiary structure. The outcropping rocks in the Erzgebirge are variable in terms of metamorphic degree. Various subdivisions have been proposed for the metamorphic rocks. Here, the proposal by Willner et al. (2000) is preferred, who recognized three major medium to high-grade metamorphic units, which are surrounded by the low-grade Phyllite Unit (Fig. 2). Two of these three units, Mica-schist – Eclogite Unit (MEU) and Gneiss – Eclogite Unit (GEU), contain abundant eclogite lenses, whereas high-pressure (HP) rocks are absent from the Red and Grey Gneiss Unit.

For detailed information on the regional geology, the map series, "Geologische Meßtischblätter", is recommended. These maps, at a scale of 1:25000, are distributed by "Sächsisches Landesamt für Umwelt, Landwirtschaft und Geologie" at Dresden. In addition, an explanatory text is available for each map. The following sheets cover the areas visited during the first part of the pre-conference excursion: GK25 5245 Lengefeld, GK25 5344 Marienberg-Wolkenstein, GK25 5345 Zöblitz, and GK25 5543 Oberwiesenthal. An overview map, Geologische Karte Erzgebirge/Vogtland at a scale of 1:100000, is also available.

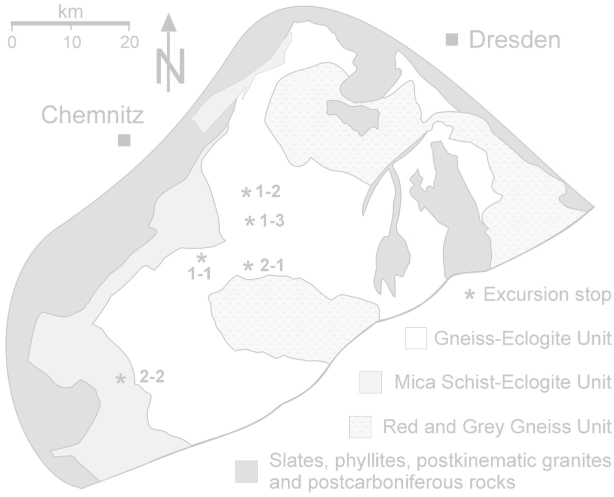

■ **Fig. 2.** Simplified geological map of the Saxonian Erzgebirge according to Willner et al. (2000). Excursion stops are shown by stars.

Stop 1-1 (Day 1). Eclogite, NW of Lauta

Coordinates: N50°40′26.6″ E13°08′08.9″

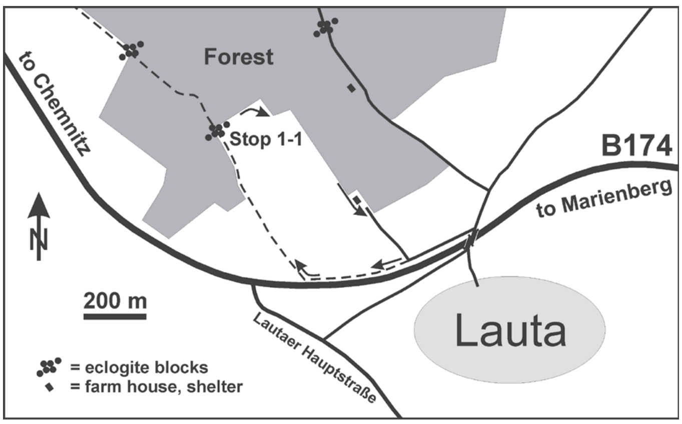

The excursion starts in the town of Marienberg. From the centre of this town go to the north-west. 2.2 km after passing the Zschopauer Tor, the old gate built in the middle of the 16th century, turn to the right, 300 m in front of the entrance of the Lautaer Hauptstrasse into the national route 174 (Fig. 3). After some hundred metres, just after passing B174 via a bridge, turn to the left and stop the vehicle after 250 m. From here walk some hundred metres first to the west and then to the north-west following a farm track to the margin of a forest (Fig. 3).

■ **Fig. 3.** Location map for stop 1-1 north-west of the town of Marienberg. The sites of eclogite boulders refer to eclogite and amphibolite lenses as mapped by Schalch (1879).

This stop is located at the northern border of the GEU with the MEU in the basement of the Saxonian Erzgebirge. In the target area boulders of fresh eclogite occur. In general, the concentration of such boulders at a specific site (see, e.g., Fig. 3) is interpreted as evidence for the existence of an eclogite body in the underground. Normally, such a body is enveloped by gneisses, which is probably the case at stop 1-1, in view of the abundant field stones of mica-schist and gneiss in the vicinity of this stop. In addition, we will find eclogite boulders by walking along the field margin, suggesting that they were sampled from the field.

A typical feature of eclogite at stop 1-1 is the homogeneous distribution of black, up to cm-sized amphibole porphyroblasts within a single boulder. These porphyroblasts have overgrown a fine-grained, equigranular matrix of garnet, omphacite, phengite, and quartz, mainly at the expense of omphacite. Massonne (1992) has studied an eclogite sample with mm-sized amphibole

Mineral	Garnet				Omphacite				Phengite				Amphibole		
Stage	I	II	IIIa	IIIb	I	II	IIIa	IIIb	I	II	IIIa	IIIa	II	IIIa	IIIb
Si	5.812	5.846	5.883	5.920	1.981	1.980	1.976	1.983	6.793	6.711	6.515	6.283	6.168	6.751	6.381
Al(IV)					0.019	0.020	0.024	0.017	1.207	1.290	1.485	1.717	1.832	1.249	1.619
Ti	0.038	0.003	0.012	0.008	0.001	0.003	0.003	0.003	0.078	0.083	0.085	0.093	0.046	0.061	0.073
Al(VI)	3.912	3.977	3.971	3.984	0.411	0.448	0.434	0.422	2.983	3.023	3.132	3.280	1.265	0.930	1.060
Cr	0.005	0.007	0.003	0.000	0.000	0.001	0.000	0.000	0.003	0.005	0.009	0.011	0.011	0.006	0.003
Fe^{3+}	0.083	0.017	0.027	0.016	0.025	0.001	0.011	0.034					0.099	0.238	0.281
Fe^{2+}	3.310	3.447	3.415	3.502	0.070	0.137	0.118	0.099	0.178	0.178	0.188	0.174	1.557	0.981	1.199
Mn	0.076	0.062	0.079	0.086	0.001	0.002	0.000	0.002	0.000	0.003	0.000	0.004	0.014	0.003	0.000
Mg	1.096	1.371	1.130	1.092	0.512	0.438	0.453	0.454	0.790	0.755	0.674	0.558	2.008	2.781	2.384
Ca	1.519	1.120	1.376	1.320	0.559	0.536	0.556	0.539	0.000	0.000	0.000	0.000	1.605	1.424	1.461
Na					0.420	0.436	0.426	0.446	0.105	0.114	0.169	0.138	0.935	0.980	1.041
K									1.716	1.729	1.703	1.672	0.214	0.127	0.166
Ba									0.014	0.027	0.021	0.021	0.002	0.000	0.000
F									0.000	0.000	0.020	0.000	0.000	0.086	0.093

■ **Tab. 1.** Representative structural formulae of minerals in eclogite sample E25d taken north-west of the village of Lauta, Erzgebirge in Saxony, according to Massonne (1992). Metamorphic stage I is the earliest (inner core compositions of garnet, omphacite, and phengite), IIIb the latest (outermost rim compositions) eclogite stage recorded by the rock. Structural formulae were calculated on the following basis: garnet: 24 O, 10 six-and eight-fold coordinated cations; omphacite: 6 O, 4 cations; mica: 42 – (Ca+Ba) valencies; amphibole: 46 valencies, 13 cations without Ca, Na, K, Ba.

porphyroblasts from this locality. This author noted a chemical zonation of garnet, omphacite, phengite, and amphibole (Table 1) and correlated the different compositions of these minerals with metamorphic stages I (early: core compositions) to III (late: rim compositions, b = outermost rim). Amphibole growth started at stage II and significantly increased in stages IIIa and IIIb. P-T conditions of the metamorphic stages were thermodynamically calculated by considering equilibria with mineral components of phengite, omphacite, and garnet (Massonne, 1992), resulting in the P-T path shown in Fig. 4. According to this path, peak pressure conditions were 2.3 GPa. Peak temperature conditions reached about 600 °C after the peak pressure event. The exhumation process, accompanied by amphibole growth, is characterized by significant cooling during decompression, a factor that might have prevented the rock from strong retrogression.

Massonne and Czambor (2007) studied the chemical bulk-rock composition of eclogites from the Saxonian Erzgebirge, including a sample from stop 1-1 (Erz02-8, see Table 2). Two groups of eclogites were distinguished: one occurring at and close to the Saidenbach reservoir, examples of which we will see and discuss at stop 1-3, and another distributed from the south-western to the central Erzgebirge, which is characterized by an N-MORB signature with a tendency towards P-MORB, as observed for the eclogite from stop 1-1.

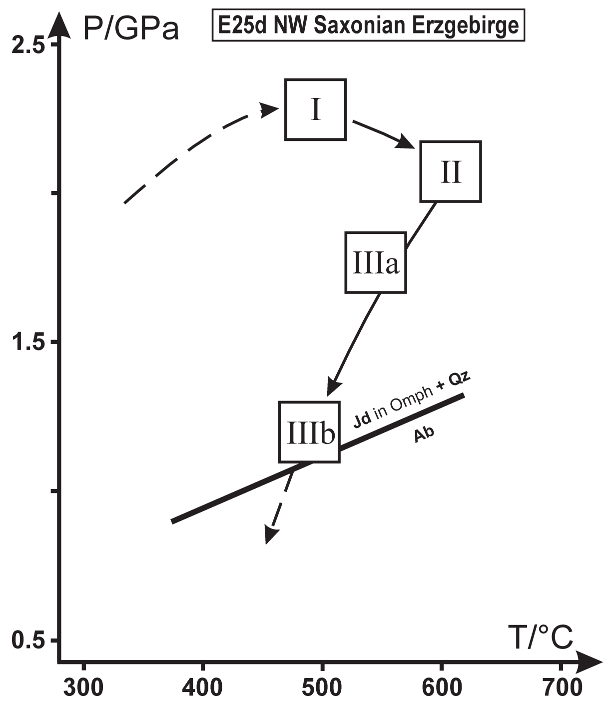

■ **Fig. 4.** P-T path derived for sample E25d (see also Table 1) from stop 1-1 according to Massonne (1992).

Site	Lauta	* Epp.	Saidenbach reservoir										Siebensäure – Meluzína			
Stop No.	1-1	1-2	1-3A	1-3A	1-3A	1-3A	1-3A	1-3A	1-3C	1-3C	1-3C	1-3D	2-2	2-2		
Sample No.	Erz02 8	E174c	E99 22	E99 23	E99 24	E99 25	E00 6	E00 17	E42 1c	E42 1d	E99 3	E42 3P	E22a	E22c	E96 15c	E95 5.3b
SiO_2 wt.%	48.00	49.50	55.75	47.53	47.40	50.60	49.12	49.92	58.54	51.17	52.13	54.83	50.84	49.74	49.56	49.91
TiO_2 wt.%	2.55	1.92	1.66	0.85	1.09	3.37	1.22	3.07	1.78	1.57	2.45	1.75	1.56	1.37	1.58	1.67

■ **Tab. 2.** Chemical compositions of eclogites from the Erzgebirge in the Bohemian Massif. The analytical data were obtained by X-ray fluorescence and, regarding some trace elements as marked in the table, ICP - mass spectrometry (Massonne and Czambor, 2007). * Epp. = 2.5 km southeast of the village of Eppendorf.

Site		Lauta	* Epp.	Saidenbach reservoir										Siebensäure – Meluzína			
Stop No.		1-1	1-2	1-3A	1-3A	1-3A	1-3A	1-3A	1-3A	1-3C	1-3C	1-3C	1-3D	2-2	2-2		
Sample No.		Erz02 8	E174c	E99 22	E99 23	E99 24	E99 25	E00 6	E00 17	E42 1c	E42 1d	E99 3	E42 3P	E22a	E22c	E96 15c	E95 5.3b
Al_2O_3	wt.%	13.55	14.80	15.80	17.63	17.38	15.28	16.55	16.23	15.88	16.48	16.43	16.13	14.48	13.92	14.19	13.64
FeO	wt.%	13.33	11.30	8.13	7.08	8.14	9.19	7.97	12.44	7.48	6.06	10.76	8.13	9.80	10.25	8.29	11.37
Fe_2O_3	wt.%			0.90			3.51				2.42					2.91	
CaO	wt.%	11.20	12.30	7.44	10.08	11.96	8.34	12.84	8.28	4.73	8.78	7.91	7.21	11.21	10.68	11.45	11.65
MgO	wt.%	5.62	6.33	4.24	8.79	8.73	4.29	8.42	4.03	3.66	5.56	4.45	4.56	7.20	6.92	6.89	6.76
MnO	wt.%	0.23	0.20	0.14	0.11	0.13	0.20	0.14	0.20	0.14	0.14	0.19	0.13	0.18	0.16	0.24	0.21
K_2O	wt.%	0.14	0.23	1.54	0.96	0.39	0.78	0.41	0.51	2.40	1.46	0.74	1.80	0.21	0.25	0.41	0.12
Na_2O	wt.%	2.53	2.32	3.30	2.28	1.69	3.21	2.33	3.49	3.31	3.43	3.37	3.40	2.89	2.99	3.06	2.84
P_2O_5	wt.%	0.27	0.12	0.15	0.22	0.14	0.79	0.15	0.84	0.16	0.28	0.45	0.24	0.11	0.08	0.09	0.11
H_20_{tot}	wt.%	0.45	0.26	0.82	0.36	0.15	0.57	0.25	0.22	0.92	1.42	0.61	0.79	0.26	1.29	0.94	0.34
CO_2	wt.%	0.21	0.13	0.12	0.34	0.55	0.10	0.25	0.11	0.18	0.30	0.16	0.20	0.11	0.33	0.02	0.15
Sum	wt.%	98.08	99.41	99.99	96.23	97.40	100.23	99.65	99.34	99.18	99.07	99.65	99.17	98.85	97.98	99.63	98.77
F	wt.%	0.04	0.03	0.04			0.05	0.04	0.04	0.03	0.07	0.06	0.06	0.07	0.05	0.07	0.09
S	wt.%	0.15	0.09	0.05			< 0.01	0.04	0.02	< 0.01	0.04	< 0.01	< 0.01	< 0.01	0.01	0.07	< 0.01
Cl	wt.%	< 0.01	< 0.01	< 0.01			< 0.01	0.02	0.01	< 0.01	0.02	< 0.01	0.01	< 0.01	< 0.01	< 0.01	< 0.01
Li	ppm ICP	53.9	22.4	36.9	32.2	14.4	14.1	11.2	16.1	31.6	21.1	26.8	34.4	35.8	23.3	16.3	14.3
Sc	ppm	54	50	27	19	36	34	47	36	26	33	33	26	52	54	52	55
V	ppm	420	353	214	138	126	317	227	317	181	207	261	203	350	320	352	361
Cr	ppm	307	298	102	263	413	47	213	83	98	204	62	86	288	357	199	181
Ni	ppm	70	95	36	150	152	21	93	37	51	47	46	43	87	80	79	81
Cu	ppm	74	69	22	72	122	37	81	30	36	48	42	29	17	17	145	122
Zn	ppm	147	116	92	63	58	128	60	136	85	83	129	93	128	87	99	106
Ga	ppm	23	20	23	16	15	24	19	24	22	19	25	25	19	16	19	19
Rb	ppm	8	13	34	13	8	18	14	15	52	41	33	58	13	8	29	12
Sr	ppm	191	114	132	474	344	173	192	262	356	164	114	216	102	58	128	78
Y	ppm ICP	69.4	39.7	29.8	16.8	9.4	37.1	18.7	55.0	26.4	25.1	53.8	28.8	45.2	44.7	40.8	35.3
Zr	ppm	162	111	158	98	79	109	77	87	206	171	139	180	90	74	86	89
Nb	ppm ICP	4.86	2.79	12.3	8.49	8.42	47.9	18.2	58.9	30.5	23.7	45.7	26.7	1.89	1.72	1.50	1.52
Sn	ppm ICP	1.29	1.27	0.65	1.06	0.66	0.32	0.27	0.00	1.03	1.07	5.85	1.88	23.9	10.7	7.20	1.61
Ba	ppm	94	42	306	2823	352	65	164	182	280	110	34	277	22		56	
Hf/Zr	ICP	0.053	0.032	0.029	0.025	0.025	0.028	0.032	0.048	0.035	0.030	0.037	0.040	0.048	0.082	0.040	0.033
Ta	ppm ICP	0.49	0.34	0.49	0.59	0.46	2.48	1.23	3.53	2.23	1.20	5.29	1.84	0.27	0.19	0.18	0.20
Pb	ppm ICP	3.46	1.59	5.05	107	11.9	1.48	3.37	4.85	10.1	1.53	8.33	4.58	0.73	1.36	6.21	10.1
Th	ppm ICP	1.59	0.16	3.97	18.2	2.63	0.07	4.48	3.63	0.57	0.31	2.45	1.73	0.33	0.27	0.19	0.08
U	ppm ICP	0.33	0.14	0.27	4.41	0.97	0.04	0.89	0.60	3.73	0.17	1.81	0.68	0.06	0.05	0.04	0.03
La	ppm ICP	14.7	4.26	14.2	111.2	35.4	11.6	19.8	35.9	9.14	15.2	29.6	15.3	4.14	4.11	2.99	2.89
Ce	ppm ICP	45.2	13.0	29.2	222.0	72.3	30.1	46.2	99.4	21.0	36.0	66.3	34.5	16.0	14.9	10.0	8.60
Pr	ppm ICP	6.86	2.13	3.99	27.9	8.75	4.97	5.37	12.3	3.11	5.43	10.5	5.12	2.82	2.56	1.83	1.77
Nd	ppm ICP	31.9	11.1	16.0	106.3	35.3	22.4	21.0	50.6	13.1	23.0	35.0	20.4	14.2	12.3	12.1	9.48
Sm	ppm ICP	9.30	4.23	4.36	23.0	8.19	5.89	4.99	10.74	3.85	6.15	10.55	5.32	4.79	3.96	4.11	3.58
Eu	ppm ICP	2.59	1.35	1.24	5.31	2.94	1.66	1.38	2.70	0.96	1.63	1.76	1.28	1.30	1.15	1.56	1.19
Gd	ppm ICP	9.26	6.86	5.25	17.9	8.91	6.81	4.28	10.13	4.80	6.32	11.60	6.10	4.85	4.40	5.39	5.36
Tb	ppm ICP	1.60	1.26	1.04	2.62	1.12	1.27	0.57	1.51	0.85	1.14	1.94	1.02	0.87	0.78	1.03	0.96
Dy	ppm ICP	10.06	6.97	6.33	8.46	4.38	7.83	3.20	9.25	5.18	6.14	10.96	5.79	5.42	4.98	6.96	6.08
Ho	ppm ICP	2.24	1.49	1.33	1.31	0.72	1.67	0.66	1.89	1.07	1.20	2.13	1.13	1.21	1.12	1.54	1.36
Er	ppm ICP	9.47	4.39	3.98	3.94	2.03	4.86	4.15	10.50	3.11	3.42	5.97	3.20	4.44	4.16	4.60	4.11
Tm	ppm ICP	0.94	0.60	0.55	0.38	0.22	0.63	0.23	0.64	0.42	0.45	0.73	0.41	0.51	0.47	0.63	0.57
Yb	ppm ICP	6.21	4.04	3.42	2.80	1.52	3.75	1.67	4.59	2.76	2.71	4.54	2.66	3.31	3.08	4.11	3.78
Lu	ppm ICP	1.03	0.60	0.51	0.35	0.19	0.56	0.29	0.78	0.40	0.41	0.62	0.38	0.56	0.51	0.76	0.57

■ **Tab. 2.** (*continued*)